

Effect of Mach number on the flame acceleration and deflagration-to-detonation transition

Wandong Zhao¹, Jianhan Liang^{1,*}, Xiaodong Cai¹, Ralf Diterding², Xinxin Wang¹

1. Science and Technology on Scramjet Laboratory, College of Aerospace Science and Engineering, National University of Defense Technology, Changsha 410073, China

2. Aerodynamics and Flight Mechanics Research Group, University of Southampton, Highfield Campus, Southampton SO17 1BJ, United Kingdom

1 Introduction

The flame acceleration and deflagration-to-detonation transition (DDT) are widely existed in safety engineering, fire system, and detonation-based propulsion devices. Over the past several decades these problems have received great attention from industrial engineers and researchers [1]. As a potential application for a detonation-based engines, the flame acceleration and DDT process are an essential and tough task on the pulsed detonation engine (PDE) and rotating detonation engine [2].

Vast efforts have been made to understand the phenomena and mechanisms associated with flame acceleration and DDT. However, most works including the experimental, numerical, and theoretical studies usually focused on the static and uniform mixtures. Whereas in terms of practical systems including safety industrial and detonation-based engines, the mixture usually has temperature, velocity, pressure, and concentration gradients. Shamsadin et al. [3] numerically studied the influence of the concentration gradient of the hydrogen mixture on the DDT and found that the lateral concentration gradient can either increase or decrease the flame acceleration, depending on the average hydrogen concentration. Ettner et al. [4] and Vollmer et al. [5] also performed numerical simulations on flame acceleration and DDT under a concentration gradient. Boeck et al. [6, 7] also conducted experimental studies on flame acceleration and DDT of a non-uniform mixture. The results showed that many mixtures were burned by turbulent deflagration after the leading detonation wave, and mixtures with higher average concentrations or lower gradients cause multi-head cellular structure. Frolov et al. [8] conducted a numerical simulation on the multi-physical working process of an aspirating PDE, including filling air, mixing, flame acceleration, and DDT processes. Studies have shown that under non-uniform mixing conditions, the mixed gas quality of the mixed gas is very unevenly distributed in the chamber. Therefore, whether there is the same mechanism of the DDT? The run-up time and distance of the DDT for a PDE under the mixture with different flighting Mach number (Ma) is still unclear, so that investigations on the flame acceleration and DDT processes in the non-uniform mixture are significantly essential for these systems.

In the present work, we investigated two kinds of flight cases including subsonic and supersonic hydrogen-air mixture flowing into the combustion chamber that generates large temperature, pressure, and velocity gradients before the mixture ignition in accordance with a lighting PDE. The reactive Navier-stokes equations with a detailed chemical reaction mechanism are used to study the flame acceleration and DDT using two-dimensional simulation with a high mesh resolution under the framework of adaptive mesh refinement (AMR) technology.

2 Computational Configuration and Numerical Methods

The illustration of the physical PDE configuration and the boundary conditions is demonstrated in Fig. 1. The PDE configuration is composed of two parts including the inlet isolation section with a size of $L_i \times L_y = 180 \text{ mm} \times 20 \text{ mm}$ and the combustion chamber with a size of $L_c \times L_y = 800 \text{ mm} \times 20 \text{ mm}$. Ten pairs of fixed solid obstructions are equipped within the chamber with a size of $d \times h = 3 \text{ mm} \times 2 \text{ mm}$, indicating that these obstacles introduce a low blockage ratio (Br) $Br=0.2$, and a slight large space interval of the obstacles is set as $S=4 \text{ mm}$ in order to yield the Mach stem easily.

An assumption of the working flight condition of the PDE located at 1KM altitude is considered in this study, and also assuming the premixed hydrogen-air mixture is flowing into the chamber with a temperature of $T=281.7 \text{ K}$ and a pressure of $P=0.09 \text{ MPa}$. Fighting conditions are set as supersonic flight $Ma=1.5$ and subsonic flight $Ma=0.8$, corresponding to case 1 and case 2, respectively. A pair of two half-cycle hot spots with slightly high energy ($T=2500 \text{ K}$ and $P=0.5 \text{ MPa}$) is used to ignite the mixture, located in the upper and lower sides of the connection part. The premixed hydrogen-air is filled with the chamber. The flowing time of case 1 and case 2 is set as $t=0.2 \text{ ms}$ that has enough time to generate a temperature, pressure, and velocity non-uniform fields, then the start time of ignition is taken as $t=0.21 \text{ ms}$ after the inlet valve is closed. The velocity inlet is used in the left side of the computation domain, whereas the no-slip and adiabatic wall is employed when the value is closed. All solid walls are taken as adiabatic and no-slip boundary conditions. The outlet flow condition is set on the left side of the domain.

The unsteady reactive two-dimensional Naiver-Stokes equations are employed to solve the multiply spices flows, flame acceleration, and DDT processes in this study, and the governed equations are given as follows:

$$\frac{\partial U}{\partial t} + \frac{\partial(F_x - G_x)}{\partial x} + \frac{\partial(F_y - G_y)}{\partial y} = S, \quad (1)$$

where U represents the vector of state parameter; F_x and F_y denote the convection fluxes; and the S denotes the source term. These symbols are further governed by the following equations:

$$U = \begin{bmatrix} \rho_i \\ \rho u \\ \rho v \\ \rho E \end{bmatrix}, F_x = \begin{bmatrix} \rho_i u \\ \rho u^2 + p \\ \rho uv \\ u(\rho E + p) \end{bmatrix}, F_y = \begin{bmatrix} \rho_i v \\ \rho uv \\ \rho v^2 + p \\ v(\rho E + p) \end{bmatrix}, S = \begin{bmatrix} \omega_i \\ 0 \\ 0 \\ 0 \end{bmatrix}, \quad (2)$$

More detailed information regarding the above parameters can be found in Ref. [9]. A hybrid Roe-HLL Riemann solver was utilized to discretize the upwind fluxes, and the MUSCL scheme together with Minmod limiter was employed to reconstruction. The diffuser term was discretized by the central difference scheme. A semi-implicit generalize Runge-Kutta scheme with fourth-order was used to the integration of the chemical kinetics. In addition, a detailed chemical reaction mechanism proposed by

Butke et al. [10] was assumed to model the reaction of deflagration and detonation flames with a wide range of pressures and temperatures.

An initial mesh grid was set as $L_x \times L_y = 4900 \times 100$, generating an equal size in both x and y directions as $dx = dy = 2.0E-4$ m. The equations above-mentioned was solved in the open-source codes in AMROC (Adaptive Mesh Refinement Object-oriented C++) with AMR approach. The AMR technique was employed, and the fourth level with refined factor (2, 2, 2) was utilized for the simulation, producing a refined mesh size of $2.5E-5$ m, which has been proved that it can generate enough mesh resolution to cope with the DDT process before this study. The cases were run on the Tianhe-1 supercomputer, where 480 cores were used to carry out this simulation, and one case took about $46080 \text{ CPU} \times \text{h}$.

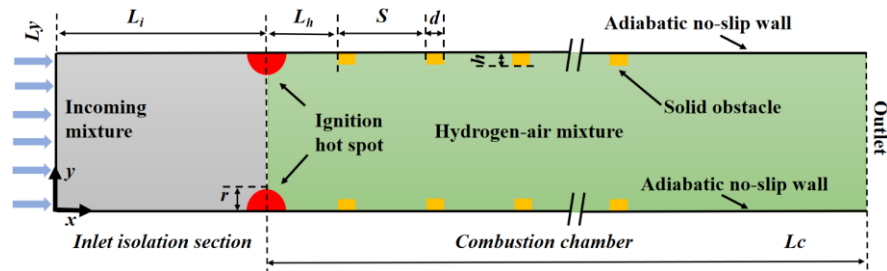


Figure 1: Illustration of the combustion configuration and boundary conditions for a PDE with supersonic and subsonic flight conditions.

3 Results

The time evolution of the flame acceleration, DDT, and detonation propagation processes for case 1 ($Ma=0.8$) and case 2 ($Ma=1.5$) is presented by Figs. 2 and 3, respectively, after the mixture ignition. Due to the flow inertia of the upstream mixture, a lot of wrinkled flames are formed owing to the Kelvin-Helmholtz instability as shown in Fig. 2(b). The flame edge passes the first obstacles quickly thanks to the high turbulent flows that produce a high flame propagation velocity. The flame edges still be separated due to the influence of the flowing inertia, until at the time of $t=0.4350$ ms that the separated flame collapse into one. Of note, a continuous compress wave is generated in the downstream tube as the flame is accelerated (see Fig. 2(g), 2(h), and (i)). Furthermore, the compress wave is gradually converged and forms a robust leading shock wave that preheats the mixture temperature that is more than $T=800$ K as shown in Fig. 2(k). At the next time, a local detonation transition is generated due to the pressure build up at the leading edge of the flame. Such a result is similar to runaway mechanism for the fast flame as confirmed by Ivanov et al. [11]. The localized donation wave passes the obstruction and survives. Hence, the detonation combustion is formed in the chamber.

In terms of case 2, due to the supersonic mixture within the chamber, a much high shock wave and high-temperature distributions are generated in the downstream chamber caused by the solid obstructions. The wrinkled flames are generated rapidly compared to case 1 at the same time of $t=0.2300$ ms. Such feature results in a large surface area of the flame front, feeding back to a large amount of energy release ratio compared to case 1. Therefore, the separated flame collapse as one with a short time. The above results also lead to a fast flame that generates

the compress wave quickly. As shown in Fig. 3(f), then the remarkable leading shock wave is produced. When the leading shock wave impacts the solid obstruction, a local detonation is generated due to the classical hot-spot mechanisms [12-14] (Fig. 3(i)). Next, a smooth detonation flame front is observed owing to the overdrive detonation as shown in Fig. 3 (j). Thanks to the overridden detonation attenuation, the flame propagation velocity reduces, and a remarkable cellular detonation structures are generated (see Fig. 3(k) and 3(l)). As compared to case 1, the run-up time in case 2 is shortened from $t=0.7400$ ms to $t=0.4450$ ms, and the run-up distance is also shortened by about 40%. Therefore, the fighting Ma number has a great impact on the flame acceleration and DDT process, and the mechanisms of the detonation ignition are also different.

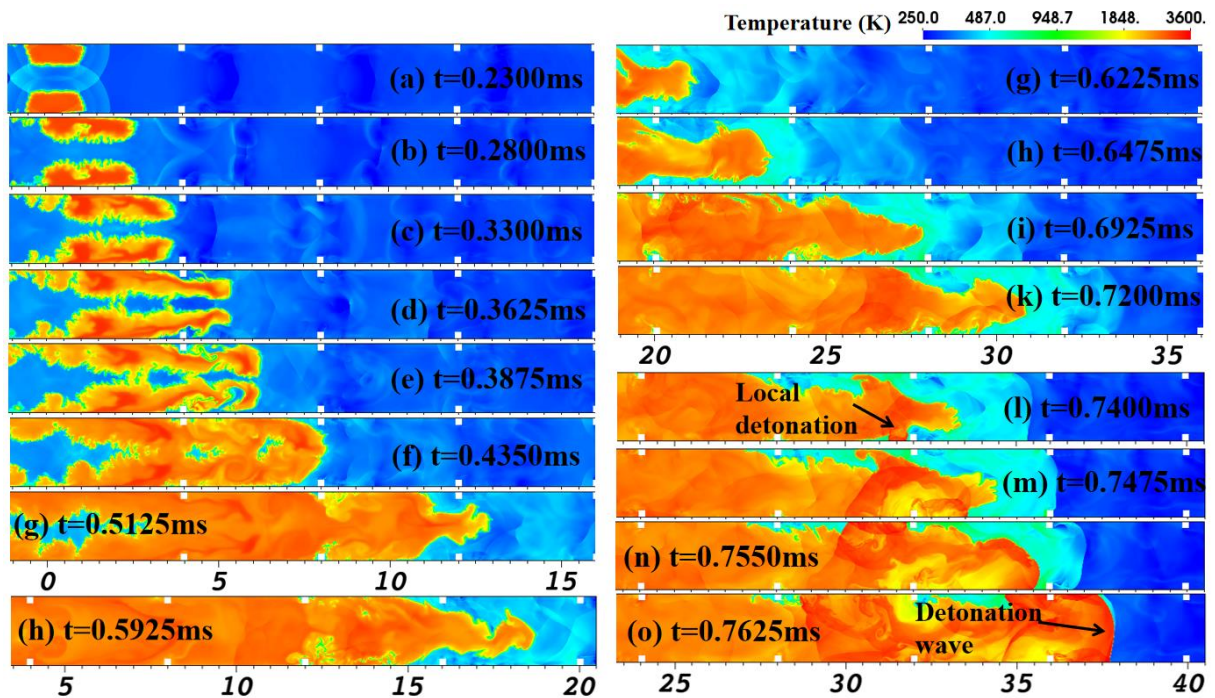


Figure 2: The snapshots of the combustion propagation under the condition of supersonic flight $Ma=0.8$.

To further compare the difference in these two cases, the pressure records in the central line within the chamber in both cases are plotted in Fig. 4 (a) and 4(b), respectively. As presented, there is more pressure fluctuation in case 2 due to the supersonic flight generating a stronger shock wave within the chamber at $t=0.2000$ ms. A gradual pressure gain is observed in the downstream tube due to the propagation of compress wave as shown lines A1 and A2, and finally, a discontinuity point is formed in both cases as shown in the black arrows, indicating that the formation of detonation wave propagates downstream. One can be observed that the maximum pressure of the overdrive detonation in the subsonic case is higher than that in the supersonic case. The maximum pressure gain ratio in the subsonic mixture is around 25, whereas the value is around 15 in the case of the supersonic mixture. Furthermore, an interesting result that the high-pressure wave propagates upstream and reflects from the inlet wall is also

observed as shown in lines B1 and B2. Such features contribute to the combustion process that propagates upstream in the regions of the inlet isolation section.

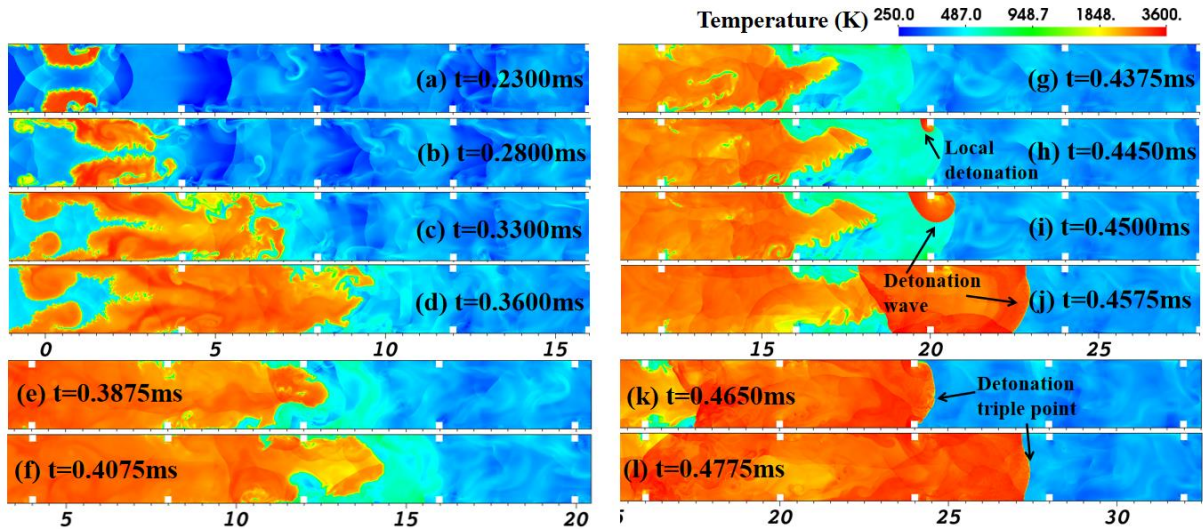


Figure 3: The snapshots of the flame acceleration and deflagration-to-detonation transition under the condition of the subsonic flight of $Ma=1.5$.

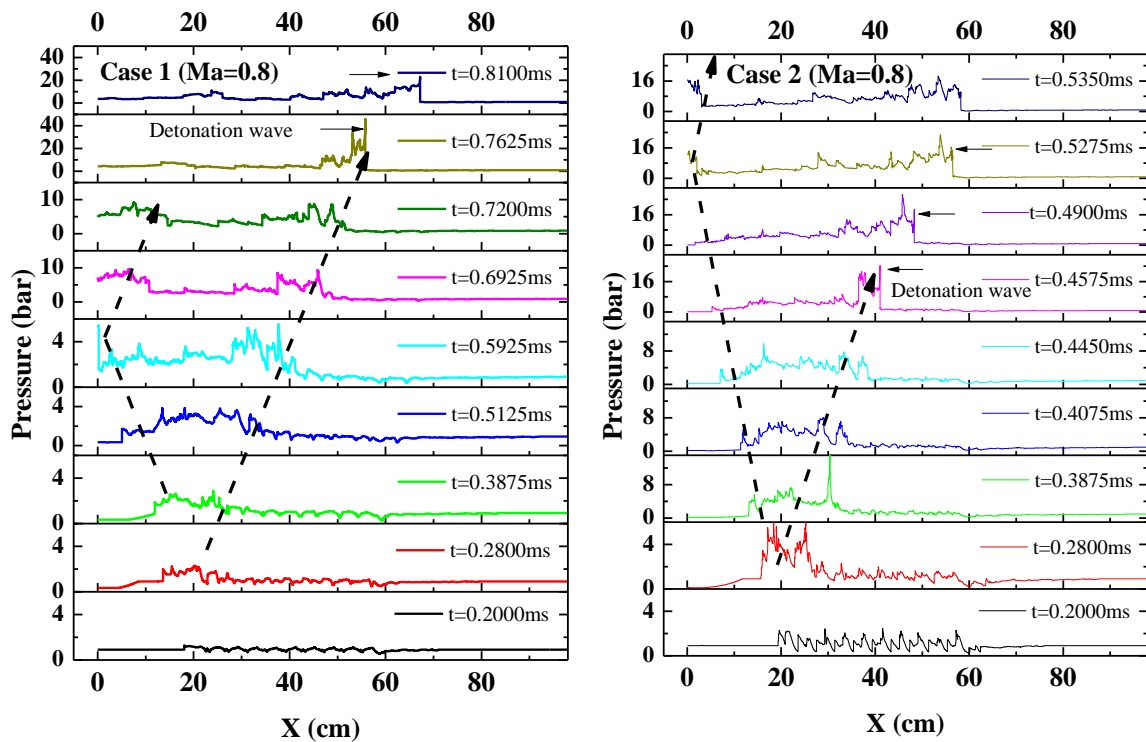


Figure 4: The pressure records in the central line of the combustion tube with time evolution for case 1 ($Ma=0.8$) and case 2 ($Ma=1.5$).

4 Conclusions

The flame acceleration and DDT processes in supersonic and subsonic mixtures were simulated by using Navier-stokes equations with a detailed chemical reaction mechanism proposed by Burke et al. [10]. Two kinds of DDT mechanisms are obtained. A classical hot spot-based DDT mechanism [12] is formed in the chamber which initially has supersonic mixture. Whereas, the onset of detonation ignited by pressure build up at the leading edge of the flame front is obtained in the combustion chamber that is filled with the subsonic mixture [11]. The run-up time and distance of the DDT in the subsonic mixture are much higher than that in the supersonic mixture; however, the value of overdrive detonation pressure gain in the subsonic mixture is much higher than that in the supersonic mixture.

References

- [1] E.S. Oran, G. Chamberlain, A. Pekalski, Mechanisms and occurrence of detonations in vapor cloud explosions, *Progress in Energy and Combustion Science*, 77 (2020) 100804.
- [2] G.D. Roy, S.M. Frolov, A.A. Borisov, D.W. Netzer, Pulse detonation propulsion: challenges, current status, and future perspective, *Progress in Energy and Combustion Science*, 30 (2004) 545-672.
- [3] M.H. Shamsadin Saeid, J. Khadem, S. Emami, Numerical investigation of the mechanism behind the deflagration to detonation transition in homogeneous and inhomogeneous mixtures of H₂-air in an obstructed channel, *International Journal of Hydrogen Energy*, 46 (2021) 21657-21671.
- [4] F. Ettner, K.G. Vollmer, T. Sattelmayer, Mach reflection in detonations propagating through a gas with a concentration gradient, *Shock Waves*, 23 (2013) 201-206.
- [5] K. Vollmer, F. Ettner, T. Sattelmayer, Deflagration-To-detonation Transition in Hydrogen-Air Mixtures with a Concentration Gradient, *Combustion Science and Technology - COMBUST SCI TECHNOL*, 184 (2012).
- [6] L.R. Boeck, J. Hasslberger, T. Sattelmayer, Flame Acceleration in Hydrogen/Air Mixtures with Concentration Gradients, *Combustion Science and Technology*, 186 (2014) 1650-1661.
- [7] L.R. Boeck, F.M. Berger, J. Hasslberger, T. Sattelmayer, Detonation propagation in hydrogen-air mixtures with transverse concentration gradients, *Shock Waves*, 26 (2016) 181-192.
- [8] Frolov, M. S., Ivanov, S. V., Zangiev, E. A., Thrust characteristics of an airbreathing pulse detonation engine in flight at mach numbers of 0.4 to 5.0, *Russian journal of physical chemistry, B.*, (2016).
- [9] X. Cai, R. Deiterding, J. Liang, M. Sun, D. Dong, Dynamic detonation stabilization in supersonic expanding channels, *Physical Review Fluids*, 4 (2019) 083201.
- [10] M. Burke, M. Chaos, Y. Ju, F. Dryer, S. Klippenstein, Comprehensive H₂/O₂ kinetic model for high-pressure combustion, *International Journal of Chemical Kinetics*, 44 (2012) 444-474.
- [11] M.F. Ivanov, A.D. Kiverin, M.A. Liberman, Hydrogen-oxygen flame acceleration and transition to detonation in channels with no-slip walls for a detailed chemical reaction model, *Phys Rev E Stat Nonlin Soft Matter Phys*, 83 (2011) 056313.
- [12] A.Y. Poludnenko, T.A. Gardiner, E.S. Oran, Spontaneous Transition of Turbulent Flames to Detonations in Unconfined Media, *Physical Review Letters*, 107 (2011) 054501.
- [13] G. Ciccarelli, S. Dorofeev, Flame acceleration and transition to detonation in ducts, *Progress in energy and combustion science*, 34 (2008) 499-550.
- [14] V.N. Gamezo, T. Ogawa, E.S. Oran, Flame acceleration and DDT in channels with obstacles: Effect of obstacle spacing, *Combustion and Flame*, 155 (2008) 302-315.